Journal of Geography, Environment and Earth Science International

Volume 27, Issue 2, Page 29-48, 2023; Article no.JGEESI.97605
ISSN: 2454-7352

Application of Geoelectric Technique in Groundwater Protection of Quaternary Aquifer in Wadi El Natrun, Egypt

Mohamed F. Bedair [a*], Rifai I. Rifai [a], Ahmed Gamal [a] and Mostafa S. M. Barseem [b]

[a] Environmental Studies and Research Institute, Sadat City University, Cairo, Egypt.
[b] Geophysical Exploration Department, Desert Research Center, Egypt.

Authors' contributions

This work was carried out in collaboration among all authors. All authors read and approved the final manuscript.

Article Information

DOI: 10.9734/JGEESI/2023/v27i2669

Open Peer Review History:
This journal follows the Advanced Open Peer Review policy. Identity of the Reviewers, Editor(s) and additional Reviewers, peer review comments, different versions of the manuscript, comments of the editors, etc are available here: https://www.sdiarticle5.com/review-history/97605

Original Research Article

Received: 05/01/2023
Accepted: 10/03/2023
Published: 14/03/2023

ABSTRACT

Qualitative and quantitative interpretations of the accessible geoelectrical resistivity data were conducted in the area located to the west of Nile Delta on both sides of the Cairo-Alexandria desert road, between latitudes 30.190816° and 30.745892° N and longitudes 29.797607° and 30.702070° E, in the northern Western Desert of Egypt. The study area is covered by thick sedimentary exposures ranging from the Miocene to the Quaternary period. Geological factors such as lithology and geological structures significantly influence the groundwater in the study area. The Quaternary, Pliocene, and Miocene eras make up the majority of strata in the study region that require water.

The study conducted twenty-three vertical electrical resistivity soundings using the Schlumberger array to define the shallow subsurface geological inferences and investigate the possibilities of finding underground water accumulations and its contamination with clay lenses. The examination of the obtained electric resistivity values revealed the segmentation of the examined section into

**Corresponding author: E-mail: md_bedr@yahoo.com;*

five geoelectrical units with lateral variations in thicknesses, lithologies, and features. The five geoelectrical units had different compositions, with the first surface unit consisting of silt clay and relatively high resistivity sands and gravels that have been altered laterally. After the surface unit, resistivity ranges from relatively modest to high. Intercalation of sand and clay occurs in the second unit, followed by lenses of relatively medium-resistance coarse sand and clay in the third and fourth units, possibly forming an aquifer, and finally relatively low-resistance sand and clay in the fifth unit.
Due to the haphazard drilling of hundreds of water wells, significant hydrogeological and environmental issues, such as soil salinization, water head decline, and groundwater salinity deterioration, have occurred. These issues have attracted significant expenditures in the field of land reclamation, both on small and large-scale projects. The study area is divided into five main geoelectrical layers observed along this cross area, as follows:
The first surface geoelectrical layer (layer A) is characterized by relatively high resistivity ranging from 8.21 to 595.3 Ohm.m. The thickness of this layer varies from 2.1 to 8.86 m. This layer represents the dry surface cover of the area and consists of gravel, sand, and silt clay.
The second geoelectrical layer (layer B) represents the dry layer lying above the water-bearing formation. It generally consists of sand and clay intercalation. The resistivity of this layer varies from 3.49 to 91.18 Ohm.m, and the thickness of this layer ranges from 17.13 to 38.3 m.
The third geoelectrical layer (layer C1) is the water-bearing formation that generally consists of coarse sand and clay. The resistivity of this layer varies from 4.41 to 37.5 Ohm.m, and the thickness ranges from 10.38 to 54 m.
The fourth geoelectric layer (layer C2) represents the lower part of the water-bearing formation. It consists of clayey sand and clay. The resistivity of this layer varies from 1.83 to 30.1 Ohm.m, and the thickness ranges from 17.78 to 31.35 m.
The last geoelectric layer (layer D) represents the lower layer of investigation, consisting mainly of clay. The resistivity of this layer is generally low, varying within a narrow range of 26.7-39.8 Ohm.m.
Finally the current study highlights the necessity of conducting in-depth geomorphological assessment studies before developing new reclamation projects, in addition to soil and water assessment.

Keywords: Vertical electrical soundings; groundwater; Wadi El Natrun; aquifer protection.

1. INTRODUCTION

Egypt is facing numerous challenges in its effort to establish and improve its towns and cities, with one of the major problems being the scarcity of water resources. In an attempt to combat this issue and revitalize rural areas, Egyptian experts are focusing on the West Nile Delta region, which is characterized by its distinctive landscape, temperate climate, uncomplicated openness, and accessibility to water sources.

One proposed strategy is to expand existing ghost towns and abandoned settlements, such as South El-Tahrir, El-Sadat City, El-Nubariya, and El-Bustan pilot zones. Moreover, the first 20 kilometers of the Cairo-Alexandria road has seen the haphazard drilling of a few water wells, upon which a few tiny private farms were constructed in the late nineteenth century.

However, this approach has led to a number of hydrogeological and environmental issues, including soil salinization, water head drop, and groundwater salinity degradation. If Egypt wishes to resolve the issue of water insufficiency, it is imperative that the country looks towards innovative solutions that take into account the environmental impact of its actions. These could include desalination, reuse of water, rainwater harvesting, and better water management systems. In addition, educational programs and awareness campaigns must be initiated to ensure the long-term success of any water-related policies.

The Wadi El Natrun aquifer in Egypt is of great importance for understanding the groundwater resources in the region. In recent years, many studies have been conducted in the area, such as those by Zarif et al. [1], Leborgne et al. [2], Ibraheem et al. [3], Salem et al. [4], Khalil [5], and Sayed et al. [6]. Geoelectrical analysis, and in particular electrical resistivity, has been the preferred method to investigate the aquifer due to its sensitivity to changes in the subsurface structure.

Despite the number of investigations already conducted in Wadi El Natrun and its environs,

there is still considerable need for further research to gain a deeper understanding of the groundwater conditions. Geophysical techniques, particularly geoelectric ones, have been found to be particularly effective in detecting the new-water/saltwater interface in aquifers. By using resistivity overviews, it is possible to obtain detailed data on the geometry, source, and overall contamination level, The West Nile Delta region's hydrogeological management can be evaluated through geoelectrical surveys, which involves collecting data about the geographical and electrical properties of the area. This data can then be used to create a map to aid decision making, as shown in Fig. 1.

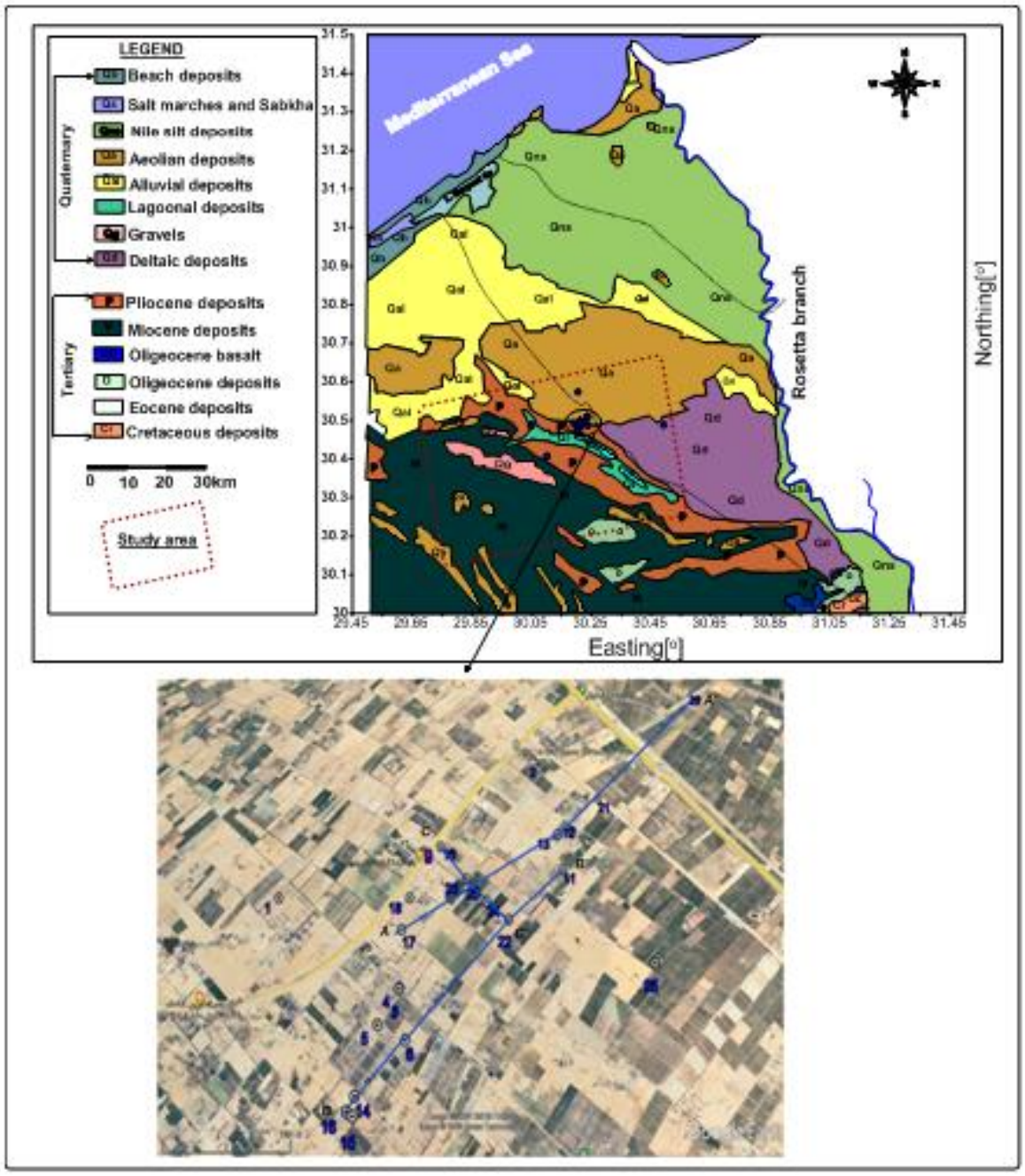

Fig. 1. Location of geoelectrical VES stations and cross sections on the geologic map (Zarif, 2009) in the area of study

1.1 Physiographic Setting

Many authors gave significant attention to the geomorphologic theories of the region west of the Nile Delta, including Sandford and Arkell [7], Said [8], Shata and El Fayoumi [9], Abu El-Izz [10], El Shazly et al. [11], Embaby [12,13] and [6]. The area of study can be geomorpholgically divided into the following units (Fig. 2) [6]:-

1. Coastal plain.
2. Alluvial plains (young alluvial plains and old alluvial plains).
3. Structural plain.
4. Tablelands.
5. Sandy plain.

The area under consideration and its subregions, as depicted in Fig. 3, have been studied and discussed by numerous authors, including Shata [14], El Fayoumy [15], Idris [16], Sanad [17], Omara and Sanad [18], El Ghazawi [19], Taylor & Jones [20], El Sabagh [21], and Sayed et al. [6]. The west of the Nile Delta is an area of great geological interest, characterized by extensive exposure of sedimentary sequences from both Tertiary and Quaternary periods. The Tertiary sediments dominate the southern and western parts of the El Ralat, Wadi El Natrun, and Wadi El Farigh depressions, consisting of sand, sandstone, clay, and limestone intercalations. The Miocene rocks are represented by the El Moghra Formation, while the Pliocene sediments have a wide distribution within the Wadi El Natrun depression and its adjoining regions, divided into Lower and Upper Pliocene. The Lower Pliocene is characterized by estuarine clay beds at the base and fluviomarine and shallow marine beds at the top, while the Upper Pliocene is characterized by shallow marine white limestone.This region has been the subject of numerous studies and research projects due to its immense geological interest. According to Said [8], the Lower Miocene arrangement consists of interbedded sand, sandstone, and clay with vertebrate remains and silicified wood and is located south and west of Quaternary deposits of Wadi El Natrun that cover wide extends of the region and are identified in water wells.

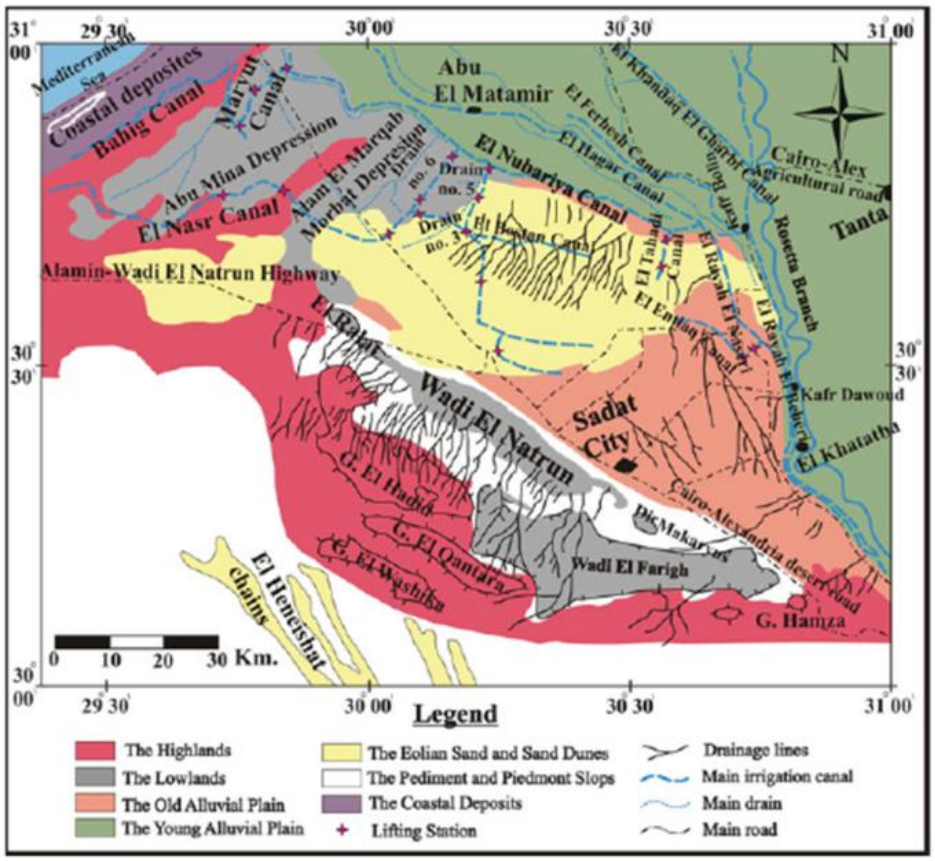

Fig. 2. Detailed geomorphologic map characterized by landforms of the study areaand its environs

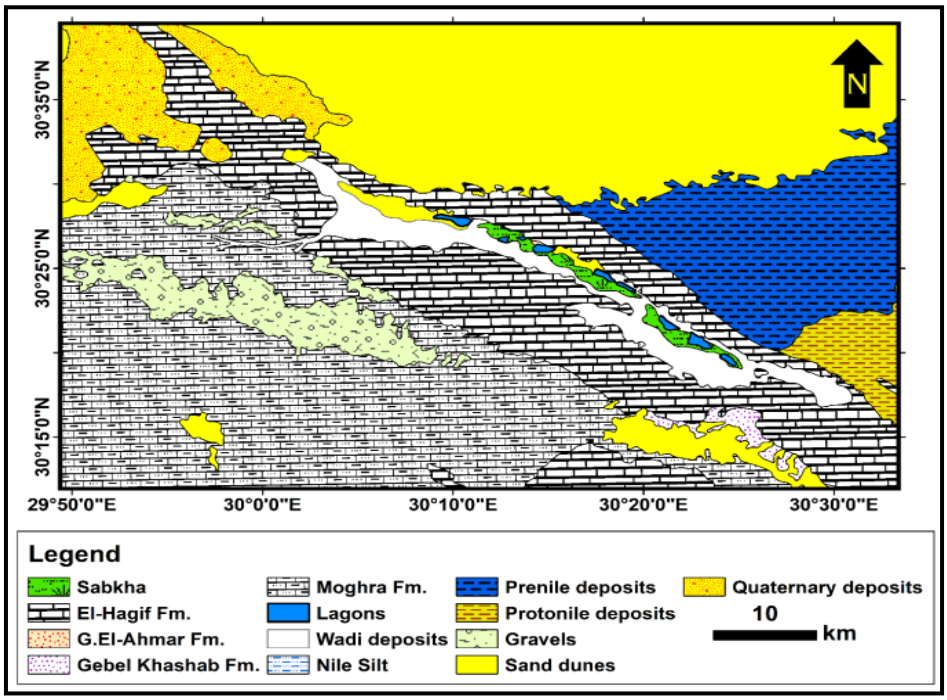

Fig. 3. Regional geological map of the study area (Conoco. 1984)

The structural aspects affecting the range and its surrounds investigated by many authors like Shata [14], El Fayoumy [15], Idris [16], Sanad [17], Omara and Sanad [18], El Ghazawi [19], Taylor and Jones [20], and El Sabagh [21]. Regarding the components that were presented, the following suggested that Northern Egypt was affected by three structural occurrences. Another event that took place in ENE (Syrian Arc) trending structures and was triggered by NW (Clysmic) or WNW 9Najd or Qattara) trending structures came before the oldest. The third structural occurrence took place in the E-W, NW (Tethyan or Mediterranean), and NNE (Aqaba) trending structures. Folds, faults, unconformities, and the shaky shelf that runs along the region's border all have a significant impact. These structural components are the foremost vital factors influencing the groundwater conditions within the area.

Several researchers, including El Fayoumy [15], Hefny et al. (1991), Sallouma and Gomaa [22], El Shikh [23], Embaby [13], Khalil et al. [24], and Massoud et al. [25], examined the groundwater characteristics of the western Nile Delta region (see Fig. 4)The groundwater of the study neighborhood is generally managed via the geological stipulations which include lithology, topography and structures. The predominant water-bearing formations associate in consequence along Quaternary (Recent then Pleistocene) below Neogene which is consist from Pliocene and Miocene. On the other hand Wadi El Natrun aqueduct's aquifers are among three distinct water-containing strata. These consist of clay-rich Quaternary alluvial sand then rock, marine sand beyond the Pliocene, and fluviomarine sand, sandstone, and clay interbeds beside Miocene. and others have separated Wadi El Natrun aquifers among Pleistocene, Pliocene and then Miocene aquifers. The Pleistocene aquifer is located of the Rosetta Department about the Nile and the eastern entrance regarding Wadi El Natrun which slants appreciably in both the eastward and northward directions. The Pleistocene stores represent the close aquifer. It instituted over about the Nile sands and hail including submission streaks on clay. The clay streaks gotten in imitation of be seriously in the direction of the upper so nicely as much calcareous stores. The aquifer thicknesses reach around 150m close Wadi El Natrun then increments regularly eastwards where it.

The shallow Pliocene aquifer found in the north is caused by surface water canal seepage that develops southward and descends to a depth of about 40 m nearby the boundary of Wadi El Natrun. The Pleistocene aquifer was classified as a tall potential aquifer by Gheorghe, A. [26]. Abd El Baki [27] The Pleistocene aquifer is

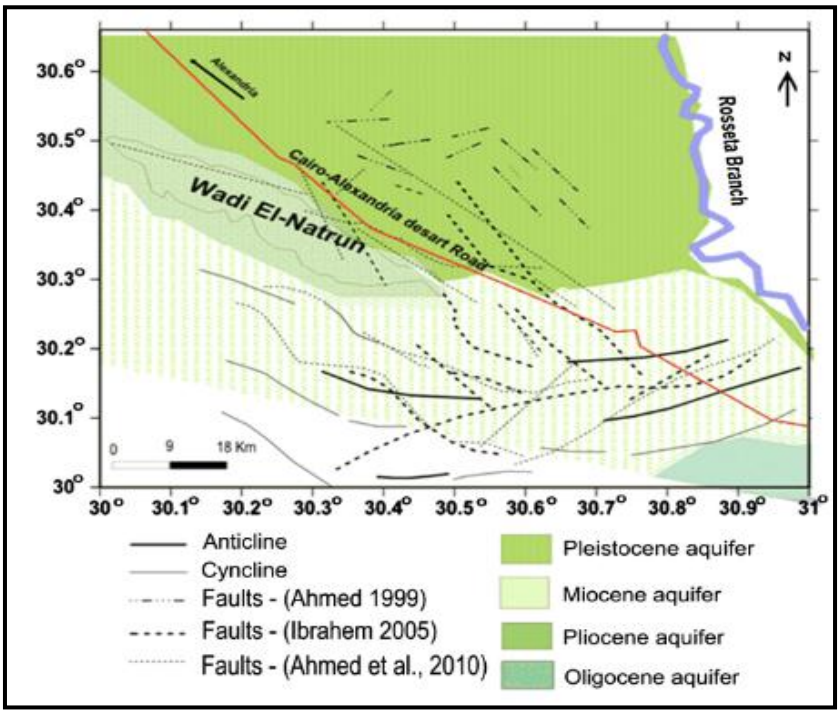

Fig. 4. Distribution of shallow aquifers in the study area and its vicinities [28,29,30,4]

specifically restricted to the Nile Delta aquifer because to the pressure-driven interaction between the two aquifers. Surface runoff from the most recent reclaimed lands, as well as the infrastructure for cloud regulation, releases additional energy. Pumps into water wells are what cause emissions to dominate. Groundwater quality in the Pleistocene aquifer ranges from pristine to barely brackish.

The study site is situated in the arid zone of Egypt where a lengthy, scorching summer and brief, mild winter are common. The climatic data for the area was gathered from the meteorological stations at Wadi El Natrun, Ganaklees, and El Tahrir. The data range from 1988 to 1998 (Zarif, 2009). The highest and lowest recorded temperatures are typically seen in January (19.4°C - 7.8°C) and Eminent (35.7°C - 21.9°C), respectively. The harsh annual precipitation concentrates progressively moves northward. It increases to 190 mm/year close to the Mediterranean shore from almost 50 mm/year in the northern part of Wadi El Natrun. The months with the most extreme precipitation are January and December, whereas the months with the lowest amounts are June, July, and Eminent [6]. Generally speaking, winter has more relative stickiness than Summer.

Based on the previous studies of the Wadi El Natrun area and its surroundings, it can be concluded that the geology of the area has a significant impact on the environment, particularly on the soil layer and groundwater. This is evident in the varying quality of groundwater and the occurrence of water logging. The changes in groundwater quality are due to the connection between the aquifers in the region and different recharge sources. The presence of clay lances in the soil layer also contributes to water logging problems and affects the quality of groundwater by increasing its salinity. The current study in the region aims to provide new data In order to foster sustainable development by environmental and hydro-geophysical studies.

2. METHODOLOGY AND DATA ACQUISITION

The Syscal Junior is an all-purpose resistivity sounding system for environmental, it can detect both resistivity and chargeability (IP). With a maximum power output of 100W at 400V, the Syscal Joiner is suitable for the majority of near-surface geophysical prospection applications, including pollution monitoring and mapping, depth-to-rock estimation, salinity management, and mapping of weathered bedrock.

The Schlumberger array's layout was used to obtain data on VES. The recorded data were

employed to ascertain the thicknesses and actual resistivities of the subsurface models based on their electrical properties [5]. There were several wells accessible at or close to the measured soundings in every case that was examined to accomplish creating the first model and calibrating the data. Following the quantitative interpretation was once employed the technique was once raised using the IPI2WIN programme. Copyright 2000, 1D interpretation regarding VES profile, the actual resistivities and thicknesses of the stratigraphic units close according to each VES status had been considered using a quantitative interpretation.

In this study, the resistivity method was utilized as it is highly sensitive to both salt and clay content, which is critical in determining the potential of groundwater as resistivity decreases with increasing salinity. The resistivity decreases when rock contains clay, as reported in several studies [31,32,33]. To better understand the underlying structures and the state of groundwater in relation to drilling data, "23" one-dimensional vertical electrical resistivity soundings (1D VES) were performed at various locations near Wadi El Natrun Alalmin road (Fig. 1). The setup of this array has been explained in previous works, including [34] (Telford et al., 1976). The VES were conducted with a maximum current electrode spacing ranging from 500 to 700 meters.

The ability of an earth medium to protect against percolating fluid by filtering and delaying it is referred to as its protective capacity and is inversely proportional to its hydraulic conductivity and Scaling with its thickness [35]. Permeability, resistivity, hydraulic conductivity, and longitudinal unit conductance show low values are typical characteristics of clay-rich materials. Therefore, it is possible to consider the protective capacity as being proportional to the longitudinal conductance (S). As a result, an overburden's protective capacity increases with increasing longitudinal conductance. The resistivity method is used to establish relationships between electrical resistivity and hydrogeological characteristics such as porosity, permeability, transmissivity, and hydraulic conductivity through the use of Dar Zarrouk Parameter - Longitudinal Conductance. This connection is based on the similarities between equations that describe the flow of groundwater through a permeable material and the flow of electricity through a conductive medium. The hydrogeological properties of an aquifer can be determined by using geoelectric measurements taken from the surface, as shown in the research by Umar et al. (2012).

Longitudinal unit conductance values of the overburden rock units in the area are used to characterize the protective capacity of the aquifer, with the longitudinal layer conductance (S) at each station being obtained through the use of an equation:

$$. T = \sum_{i=1}^{n} \frac{h_i}{\rho_i}$$

Where hi is the layer thickness, ρ_i is layer resistivity while the number of layers from the surface to the top of aquifer varies from i= 1 to n

While the transverse resistance (T) was obtained from the equation:

$$T = \sum_{i=1}^{n} hi\, \rho_i$$

It can be concluded that the protective nature of the overlying layer of an aquifer is dependent on the relationship between its thickness and resistivity. The transmissivity of the aquifer can be estimated by multiplying the hydraulic conductivity by the layer's thickness. Transverse resistance (T) depends on product of the resistivity and the thickness as well as the hydraulic conductivity [36]. Clay layers have lower resistivities and hydraulic conductivities, which corresponds to a lower transmissivity level. Thus, it is reasonable to assume that the protective quality of the overburden is in direct proportion to the thickness and resistivity of the layer.

The topographic survey is carried out to determine the locations (latitudes and longitudes) of the sounding stations on the topographic map by using the GPS apparatus (Trimble type) contact with nine satellites.

3. RESULTS AND DISCUSSION

The geoelectrical data can be more effectively understood when they are presented in the form of contour maps and cross sections. Contour maps demonstrate the lateral variation of a particular parameter such as depth or resistivity, across the study area. Cross sections provide an understanding of the complete layering of the area with depth along a particular direction.

These forms of presentation provide a clearer picture of the underlying structure of the area. An example of this is shown in Fig. (5), which displays the interpretation of the modeled resistivity data from sounding VES No. 12 near a well. The vertical geoelectrical section of the area is believed to consist of five geoelectrical layers.

1- A surface geoelectrical layer “A” which is characterized by relatively high resistivity values range from 8.1 to 595.3Ohm.m. The thickness of this layer varies from 2.1 to 8.86 m. This layer represents the dry surface cover of the area and consists of Gravel, sand and silty clay.

2- A dry geoelectrical layer “B” overlying the water-bearing formation represents the dry layer lying above the water-bearing formation. It consists generally of Sand and clay intercalation. The resistivity of this layer varies from 3.49-91.18 Ohm.m. The thickness of this layer shows range from 17.13 to 38.17m.

3- A saturated geoelectrical zone (C) that divided in to two layers (C1 & C2) according to resistivity values as follow:

a) The upper part of the water-bearing formation, geoelectrical layer “C1” is the water-bearing formation consists generally of coarse sand and clay. The resistivity of this layer varies from 4.41 to 37.5 Ohm.m. The thickness of this layer varies from 4.41 to 54 m.

b) The lower part of the water-bearing formation, geoelectrical layer “C2”) represents the lower part of the water-bearing formation. It consists of clayey sand and clay. The resistivity of this layer varies from 1.83 to 30.1 Ohm.m . The thickness of this layer varies from 17.78 to 31.35 m..

4- The last geoelectrical layer “D” represents the lower layer of investigated section. It consists mainly of clay. The resistivity of this layer is generally low and varies within a narrow range (6.44 – 39.8 Ohm.m.).

A detailed description from geoelectrical parameters (resistivity & thickness)of each layer from top to bottom is given in Table (1) as follows.

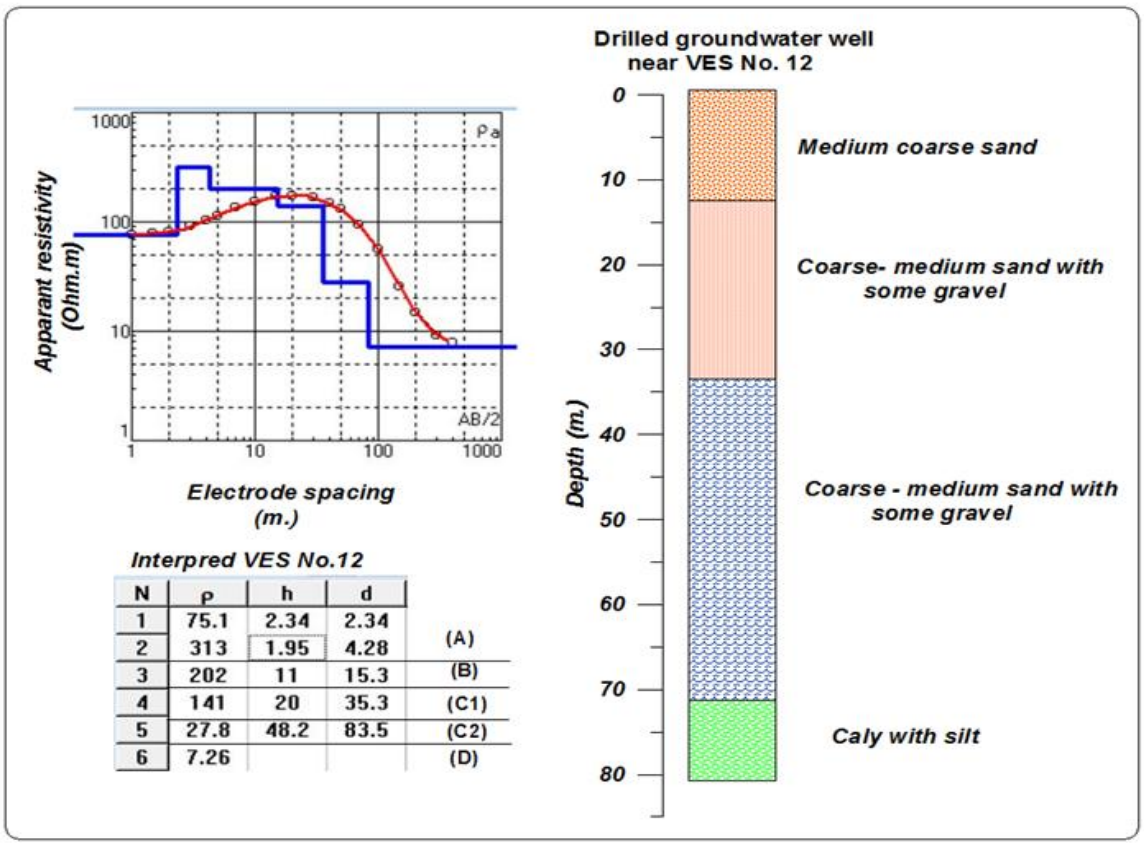

Fig. 5. Interpreted VES No 12 and the data of the near drilledgroundwater in the study area

Table 1. Thickness and resistivity ranges of the different geoelectrical layers

Geoelectrical layer		Resistivity (Ohm.m)		Thickness(m.)		Desribtion
		Min.	Max.	Min.	Max.	
(A)		9.2	376.5	3.28	8.86	Gravel, sand and silt clay
(C)	(C1)	4.41	37.5	10.83	54	Coarse sand and clay
	(C2)	1.83	25.44	17.78	34.8	Clayey sand and clay
(D)		6.44	39.8	***	***	Clay & silt

The geoelectrical layers gotten from the interpretation of the sounding curves have been sequenced through cross sections in terms of thickness and resistivity ranges. Such geoelectrical cross areas would complete the picture of the subsurface, and outline the level variation in thickness of the diverse geoelectrical layers along specific directions.

3.1 Geoelectrical Cross-sections

The outcomes of the quantitative analysis and interpretation of geoelectrical resistivity sounding are used to construct three geoelectric cross-sections that represent the variation of layers according to their resistivity values. Five geoelectrical cross-sections have been measured in trends A - A`, B - B` and C - C` are shown in Figs. 6, 7 & 8 respectively as follow:

1- Cross section A-A`

The cross section A-A' runs in the SW-NE direction (Fig. 6). Includes the VES stations V17, V25, V13, and V20. The following four major geoelectrical strata are seen along this crossing area:

A surface geoelectrical layer (layer A) it is characterized by relatively high resistivity range from 44.7 to 162.2 Ohm.m. The thickness of this layer varies from 4.2 to 5.6 m. This layer corresponds to the arid surface covering of the region and is composed of a mixture of gravel, sand. The geoelectrical layer immediately below it (known as layer B) signifies the dry layer located atop the water-containing stratum. Typically, it is made up of alternating layers of sand and clay. The resistivity of this layer varies from 22.2 to 44 Ohm.m . The least resistivity value of this layer is found at VES station V20 (22 Ohm.m), The thickness of this layer varies from 29 to 32.7 m. The third geoelectrical layer (layer C1) is The water-containing stratum exists generally of coarse sand and clay. The resistivity of this layer varies from 8.1 to 24.1 Ohm.m . The least resistivity value of this layer is found at VES station V25 (10.6 Ohm.m), the thickness of this layer varies from 27 to 46 m. The fourth geoelectric layer (layer C2) represents the lower part of the water-bearing formation. The resistivity of this layer varies from 2.8 to 11.7 Ohm.m . The least resistivity value of this layer is found at VES station V25 (5.8 Ohm.m).

2- Cross-sections B-B`

This cross section is constructed along the SW-NE direction cross section A-A` (Fig. 7). It incorporates VES stations V6, V11, V14, V16 and V22. Four main geoelectrical layers are observed along this cross area as follows:

Layer A is the uppermost geoelectrical layer with a resistivity ranging from 44.7 to 376.5 Ohm.m and a thickness ranging from 5.2 to 8.8 m. It is composed of a mixture of gravel, sand, and silt clay and signifies the dry surface covering of the area. Layer B, located directly below layer A, is also a dry layer that lies atop the water-containing stratum. It is generally comprised of sand and clay intercalations with a resistivity varying from 11.6 to 39.3 Ohm.m, and a thickness ranging from 17.1 to 29 m. The third layer, layer C1, represents the water-bearing formation and consists of coarse sand and clay with a resistivity range of 4.4 to 87.7 Ohm.m. This layer's thickness varies from 23 to 45.9 m, and its least resistivity value is identified at VES station V16 (4.4 Ohm.m). The fourth layer, layer C2, is the lower part of the water-containing formation and is made up of clayey sand and clay. It has a resistivity range of 1.3 to 11.2 Ohm.m, and the layer's lowest resistivity value is found at VES station V22 (1.3 Ohm.m).

3- Cross-sections C - C`

This cross section is constructed along the S-N direction cross section A-A` (Fig. 8). It incorporates VES stations V9, V10 , V23 , V25, V24 and V22 . Five main geoelectrical layers are observed along this cross area as follows:

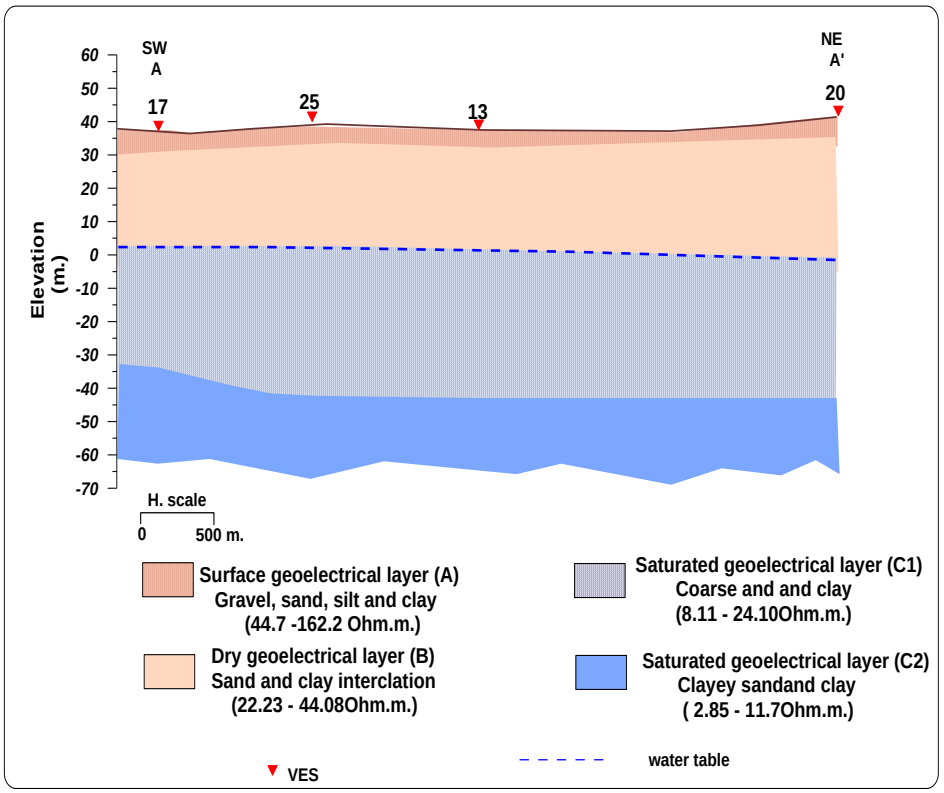

Fig. 6. Geoelectrical cross-sections A-A`

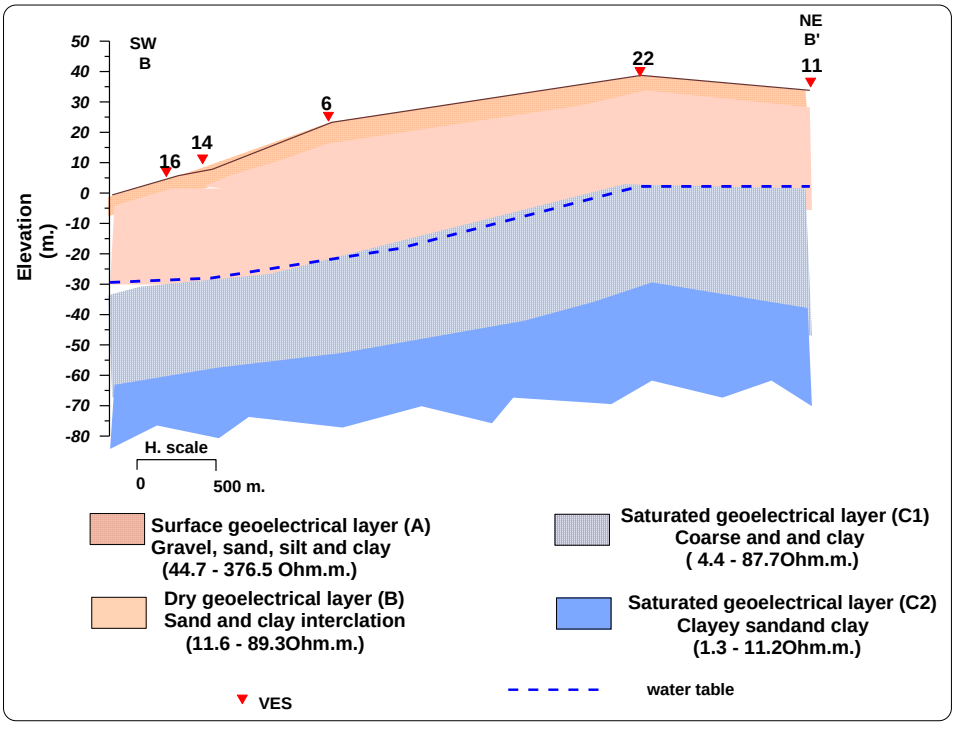

Fig. 7. Geoelectrical cross-sections B-B`

A surface geoelectrical layer (layer A) which is characterized by relatively high resistivity range from 21.4 to 44.7 Ohm.m. The thickness of this layer varies from 4.4 to 5.2 m. This layer represents the dry surface cover of the area and consists of Gravel, sand and silt clay. The second geoelectrical layer downwards (layer B) represents the dry layer laying above the water-bearing formation. It consists generally of Sand and clay intercalation. The resistivity of this layer varies from 11 to 44 Ohm.m . The least value for resistivity in this layer is observed to be at VES station V24 (11 Ohm.m), The thickness of this layer varies from 29 to 37 m. The third geoelectrical layer (layer C1) is the water-bearing formation consists generally of coarse sand and clay. The resistivity of this layer varies from 8.1 to 13 Ohm.m . The least resistivity value of this layer is found at VES station V22 (8.1 Ohm.m), The thickness of this layer varies from 25.8 to 46.8 m. The fourth geoelectric layer (layer C2) Indicates the basal region of the water-bearing formation. It consists of clayey sand and clay. The resistivity of this layer varies from 2.8 to 9.7 Ohm.m . The least resistivity value of this layer is found at VES station V22 (2.8 Ohm.m). The last geoelectric layer (layer D) represents the lower layer of investigation. It consists of mainly clay. The resistivity of this layer is generally low and varies within a narrow range (2.8 – 9.7 Ohm.m.).

3.2 Groundwater Conditions

The research area is dominated by Pleistocene and Miocene aquifers. A contour map of water depth was produced (Fig. 9) and it only shows the estimated depths to the top of the water-containing formation. The map is useful for determining the water depth in areas where new dry wells are planned to be drilled and is significant for the region's growth in agriculture or industry that relies on its groundwater supply. The map indicates that the area with the shallowest water depth (22.7–42.3m) is located in the center of the research region. The water depth gradually increases towards the northern and eastern boundaries. This can be assigned to the variation in the area's surface geography. As a result, the central part of the area with a depth of 34m is the preferred location for drilling new wells.

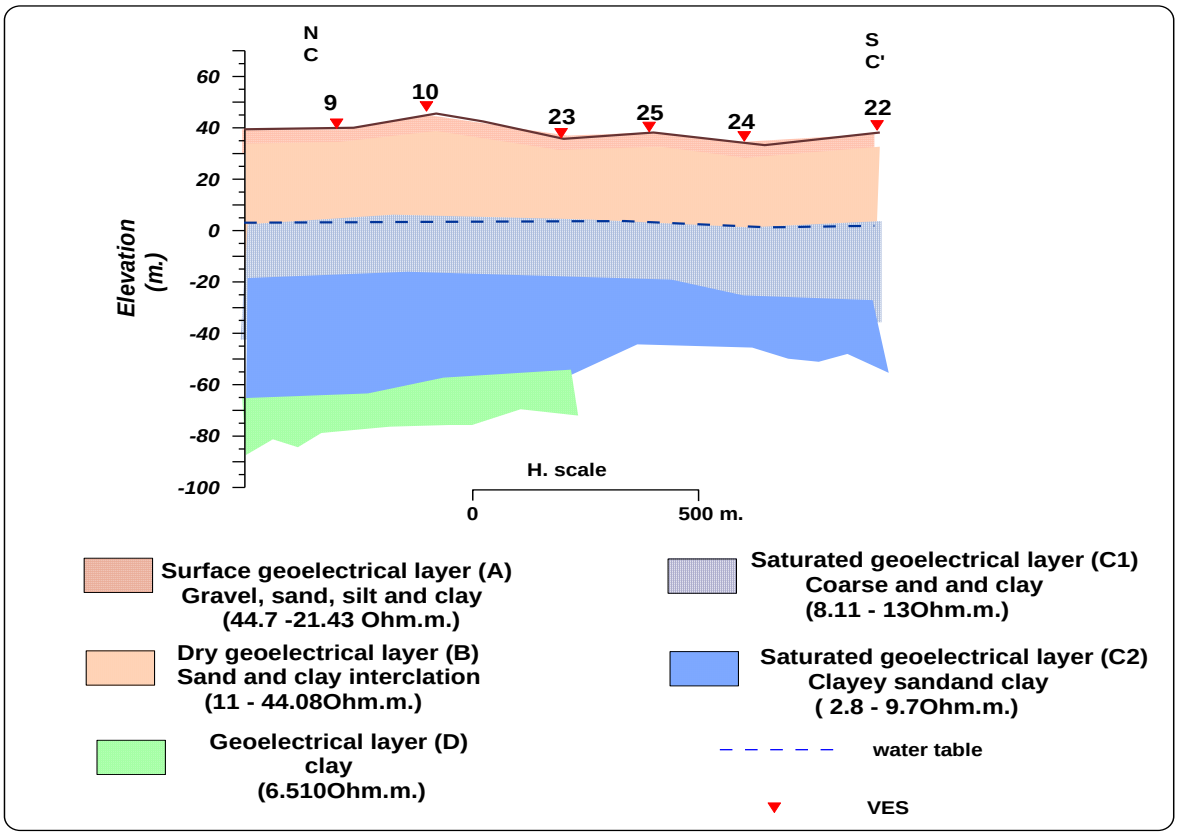

Fig. 8. Geoelectrical cross-sections C-C`

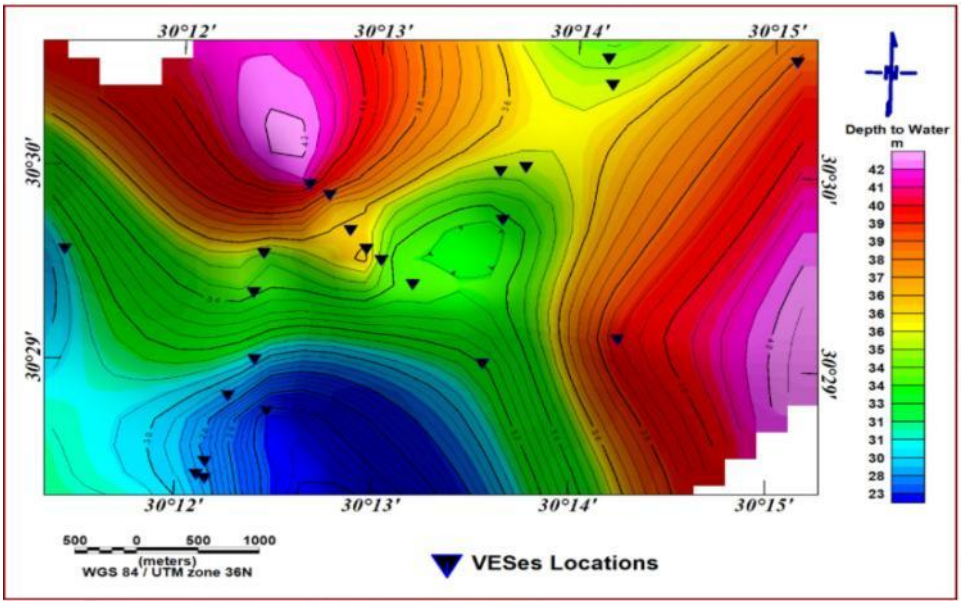

Fig. 9. Depth to water contour map in the study area

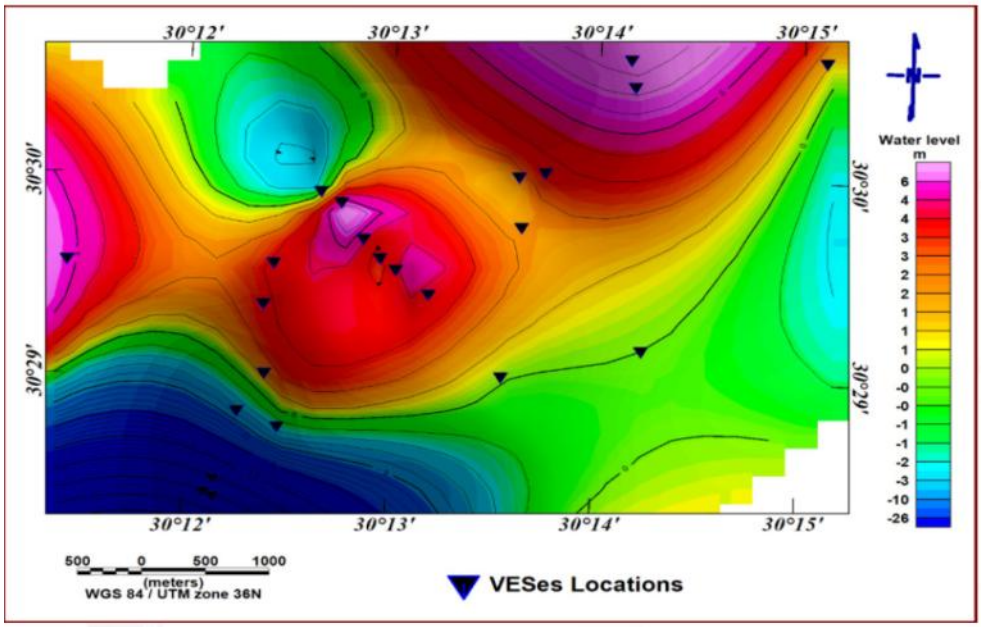

Fig. 10. Water table contour map in the study area

With the objective of identifying the lithology of the saturated geoelectrical zone, located below the water table, which could indicate layers of the underground with larger or smaller capacity of protection to contaminants, a resistivity map was elaborated. This map refers to the geoelectrical level, whose top was determined by the position of the water table, separating the dry portion of the saturated. The Water table contour map appeared in Fig. (10) was constructed using the upper surface of water-bearing formation related to sea level. The water table is shown on the map to be between 2.9 and -34 m., and in the most areas of the region, the usual water powered sharp is around 3.5 m.

3.3 Saturated Geoelectrical Zone

According to the interpretation of geoelectrical data, it found that the saturated zone (C) in divided in two layers (C1 & C2). The layer (C1) represents the upper part of the water-bearing

formation. This layer's 1soresistivity (Fig. 11) is modest and has a restricted range (4.4 to 37.5 Ohm.m.). This can be attributed to the lithologic nature of the stratum, which is comprised of coarse sand and clay on the one hand and high-quality water on the other. The typical resistivity of this layer falls within this low resistivity range and is less than 10 Ohms in most of the area's western and southern regions.

The iso-pach map (Fig. 12) shows that thickness that grows at the southern, western, and northeastern portions of the area under study, reaching a thickness of 54 m, while the northwestern and eastern portions are distinguished by a smaller thickness of around 10.8 m. The groundwater's topmost layer is represented by this unit, where clay and coarse sand make up the lithology of this stratum.

The saturated geoelectrical layers (C2) represents the lower part of the water-bearing formation. The resistivity of this layer (Fig. 13), which is low and has a constrained range (1.8 to 25.4 Ohm.m.). This can be attributed to the lithological composition of clayey sand and clay on the one hand, and the quality of water saturating this layer on the other. Here in the southwest, particularly where the resistivity is less than 1.8 Ohm.m, the impact of lagons is evident. The typical resistivity of this layer a fall within this low resistivity range and is less than 10 Ohms in most of the area's western and southern regions.

According to (Fig. 14), the area of study's thickness grows in the southwestern, western, and northeastern regions, where it reaches 34.8 metres. In contrast, the area's northwestern and eastern regions have a thinner thickness of around 17.7 metres. This unit corresponds to an aquifer containing brackish or salty groundwater, and its lithology is made up of sandy clay. Lagoons, one of the primary sources of recharge, have an impact on water salinity.

3.4 Aquifer Protective Capacity

The values of the first layer resistivity can be used to create corrosivity maps that are used to assess the level of soil corrosivity at shallow depths in the area (Fig. 15). Corrosive regions are those with comparatively low resistivity values, and non-corrosive regions are those with high resistivity values [37]. The principal natural defense against pollution in granular and unconfined aquifers is connected to the presence of overlapping clay layers, whose capacity for protection is limited by the delay in the penetration of solutions because of their poor permeability. According to [38], the protection level of an aquifer can be thought of as directly proportionate to the relationship between thickness and resistivity. Figuring out the aquifers' geo-electric properties, then utilizing that knowledge used to calculate the soil corrosivity and aquifer protective capacity.

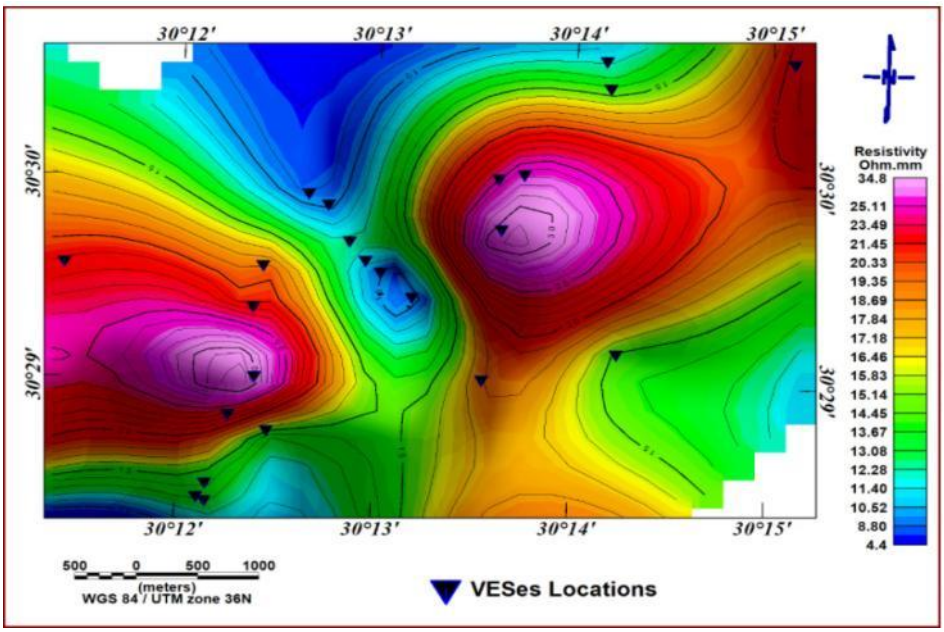

Fig. 11. Iso-resistivity contour map of the geoelectrical layer C1

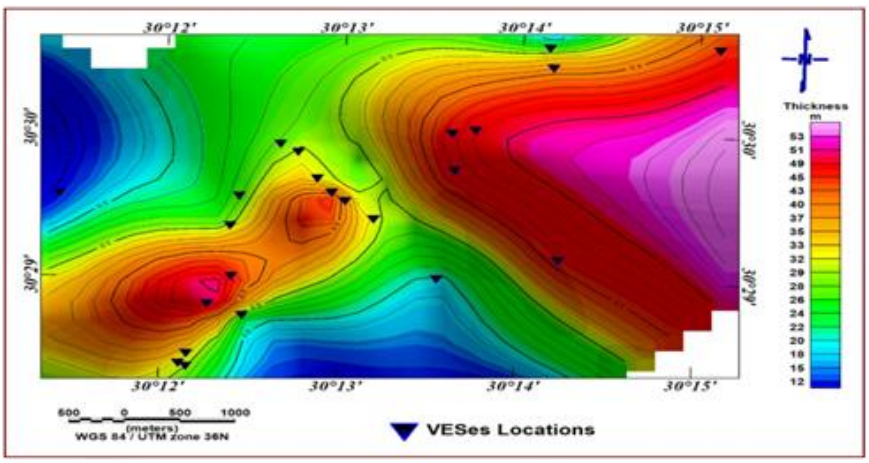

Fig. 12. Iso-pach contour map of the geoelectrical layer C1

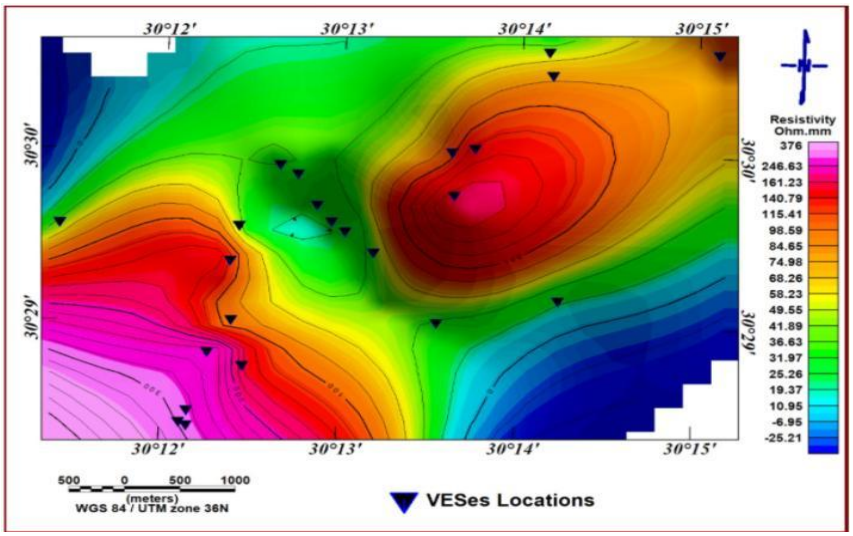

Fig. 13. Iso-resistivity contour map of the geoelectrical layer A

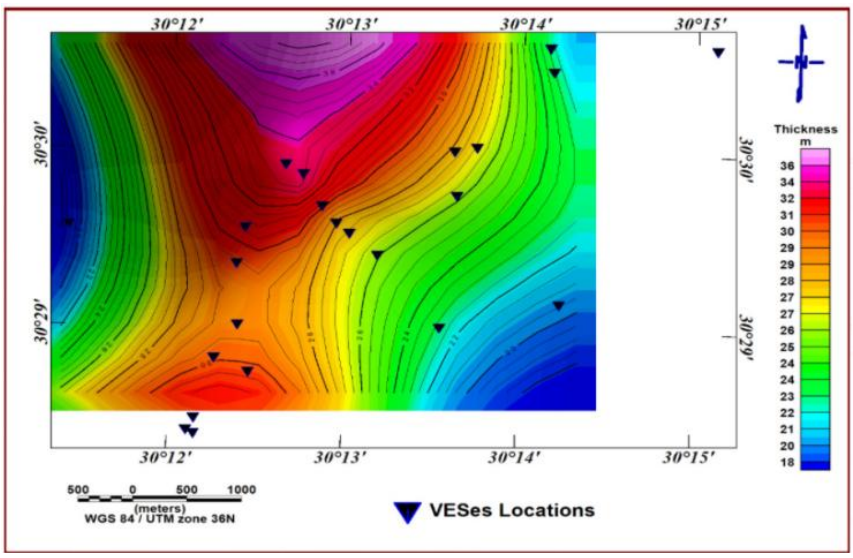

Fig. 14. Iso-pach contour map of the geoelectrical layer C2

Table 2. Classification of soil resistivity in terms of corrosivity [after Baeckmann and Schwenk [39], Agunloye [40], and Oladapo et al. [41]]

Sil resistivity (ohm-m)	Soil corrosivity
10	Very Strongly Corrosive (VSC)
10-60	Moderately Corrosive (MC)
60-180	Slightly Corrosibe (SC)
> 180	Practically Non- Corrosive (PNC)

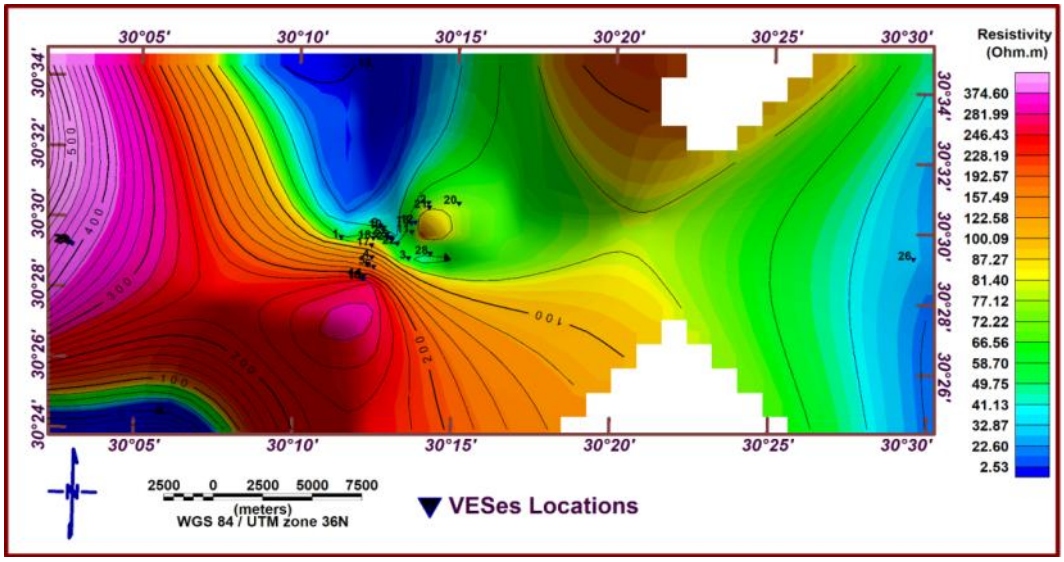

Fig. 15. Iso-resistivity contour map of the geoelectrical layer A

On the other end of the range are clay soils, particularly those affected by contaminated substance. Table (2) presents a classification of soil resistivity according to corrosivity.

The distribution of electrical resistivity across the forest layer is shown in Fig. (15). This layer extends from the surface to a depth ranging from 2.1m. to 8.8m. This layer is lithologically composed of gravel, sand, silt and clay. This composition is well reflected through the wide range of resistivity (8.21 to more than 595Ohm.m.). The resistivity values smaller than 40 ohm.m are associated predominantly with clay sediments (clay-sand and clay) and moderately to strongly corrosive. The transition from clay to sand is gradual as increase resistivity values, presenting intermediary layers of clay-sand and sand-clay sediments also, practically non corrosive. Generally, Areas characterized by relatively low resistivity values are considered corrosive while areas with high resistivity values are considered non-corrosive n [37].

In order to ascertain the aquifer protective, transmissivity and soil corrosivity of the area under consideration, the longitudinal conductance for overburden layers to saturated zones and transverse resistance values for saturated zone were evaluated from the measured resistivity values and the thicknesses of the layers. Excellent conductance values in the longitudinal direction correspond to high values very good and good Aquifer Protective Capacity (APC), low longitudinal conductance values are associated with poor and weak (APC) are presented in Table (3).

The thickness of the resistivity results is defined as transverse resistance (T) (Fig. 16). Based on empirical evidence, it can be concluded that the transmissivity of an aquifer is proportional to its transverse resistance [43,44]. Clay layers are associated with low resistivity and low hydraulic conductivity, while high resistivity is linked to high hydraulic conductivity. Therefore, the protective capacity of the overburden can be evaluated based on the ratio of thickness to resistivity. The transverse resistance map shows that high values of (T) (>400 ohm.m2) are found in zones of high transmissivity in the southern part of the study area [45-50].

Table 3. Longitudinal conductance/ aquifer protective capacity rating [Oladapo et al. [41] and Adeniji et al. [42]]

Longitudinal conductance (mhos) rating	Aquifer protective capacity
> 10	Excellent
5-10	Very good
0.7-4.49	Good
0.2-0.69	Moderate
0.1-0.19	Weak
< 0.1	Poor

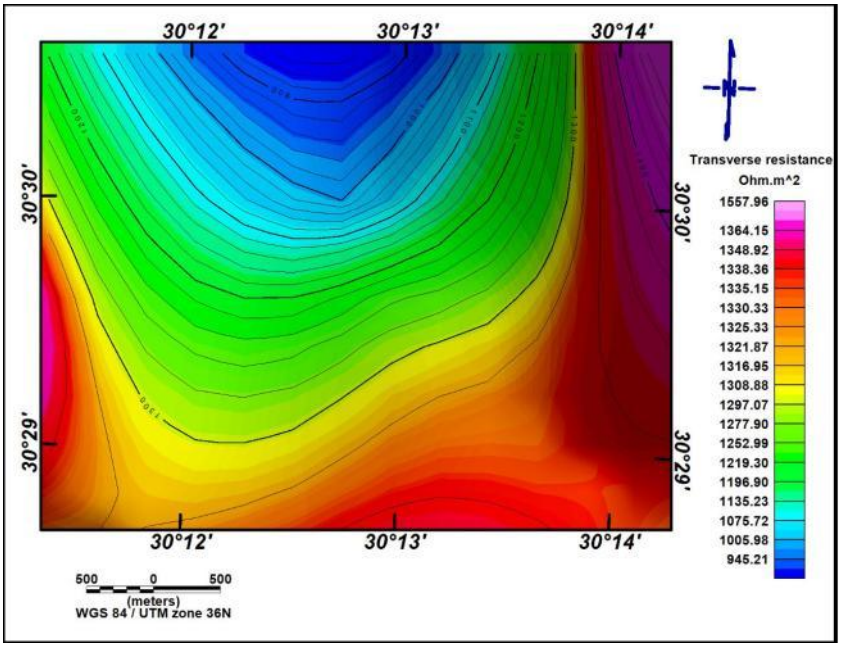

Fig. 16. Transverse resistance map

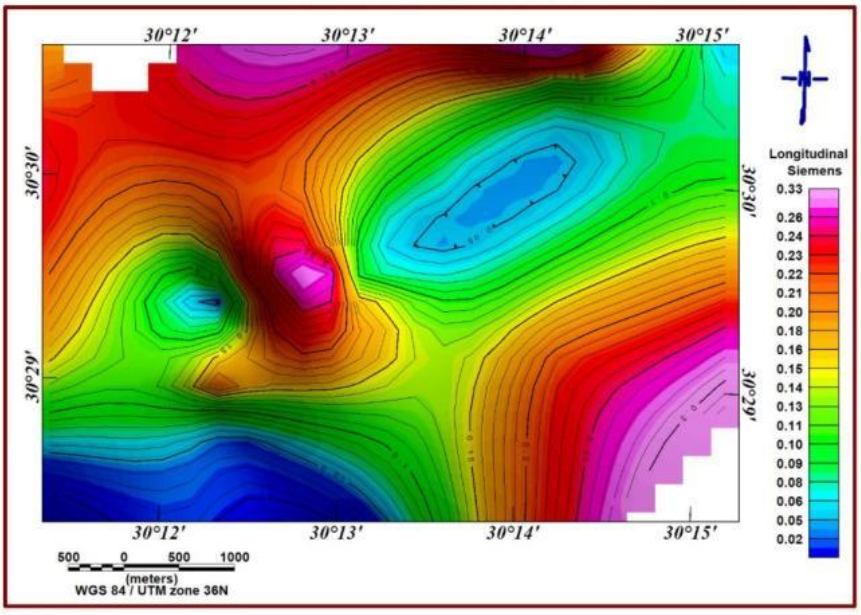

Fig. 17. Longitudinal conductance map

The map of longitudinal conductance (Fig. 17) illustrates the protective capacity of the overburden layers on the saturated zone. In this illustration, values of S > 1.0 siemens would indicate zones in which the aquifer would be protected. In comparison, values of S < 1.0 siemens would indicate zones of probable risks of contamination. According to Table (3) the rating of longitudinal conductance is > 2 the aquifer protective capacity is moderate to excellent that observed in the northwestern and southeastern of the study area. When, the rating of longitudinal conductance is < 2 the aquifer protective capacity is weak to poor that observed in the central and southwestern part of the study area [46-56].

4. CONCLUSION AND RECOMMENDATION

The results of the quantitative interpretation of the geoelectrical resistivity sounding data have been used to create five cross-sections which show how the strata vary in terms of their resistivity values. Three subsurface sections, each made up of five geoelectrical layers, have been measured along the trends (A - A', B - B', and C - C'). The presence of groundwater in the study area was identified using information from a drilled well and the results of the geophysical interpretation. According to the analysis, the center of the area is expected to have a shallow depth of water (22.7-41.4m). The water depth increases in other parts of the area, reaching 40-60m near the northern and eastern boundaries. This can be attributed to the changes in the surface geography of the area. As a result, the central section of the area with a 34-meter depth is preferred for drilling new water wells.

The results of the study reveal that the water-bearing layer in the research area is the thickest in the center with a maximum thickness of 46.8 meters and gradually decreases towards the south, reaching a thickness of 8.86 meters. The water table in the area ranges from 8.6 to -22.7 meters and the gradient of the water flow is typically around 3.5 m/km. The primary aquifer in the region is made up of Pleistocene layers of Nile sands and gravels with occasional clay layers. In the north, there are more occurrences of calcareous deposits and clay streaks. The thickness of the aquifer in the area near Wadi El Natrun is approximately 150 meters and gradually increases to about 300 meters as it moves to the east. Most of the groundwater in the Pleistocene aquifer is either semi-confined or in a free water table state, and the water table has an east-west and north-south gradient.

Although there are sources of contamination on the surface, aquifers are likely to form a direct pathway for contamination. This study indicates that future development projects can be constructed in first-class districts without worrying about aquifer contamination, but that businesses and other projects should be established with extreme caution in the location. The transverse resistance map shows high values of (T) (> 400 ohm.m^2) can be associated with zones of high transmissivity that exist in the southern part of the study area. Finally, the rating of longitudinal conductance is > 2 the aquifer protective capacity is moderate to excellent that observed in the northwestern and southeastern of the study area.

From the above mention, it can be recommended the following items:

1. Government, individuals or estate developers who wish to site borehole within the study area are strongly advised to consider the VES points at the central part of the study area.
2. Laboratory checks can be conducted in order to access the protective capacity of aquifers within regions described as poor and weak before carry any form of activity there.
3. Areas with poor aquifer protective capacity should be avoided for sinking borehole to reduce leachates infiltration to the groundwater.
4. Plastic pipes are more preferable in the areas of good and moderate aquifer protective capacity.

COMPETING INTERESTS

Authors have declared that no competing interests exist.

REFERENCES

1. Zarif FM, Elshenawy AM, Barseem MSM, Al-Abaseiry AA, Sayed ANE. Evidence of geoelectrical resistivity values on groundwater conditions in Wadi El Natrun and its vicinities, West Delta, Egypt (cases studies). Sci Rep. 2022;12(1):10745.
DOI: 10.1038/s41598-022-12644-0, PMID 35750674.

2. Leborgne R, Rivett MO, Wanangwa GJ, Sentenac P, Kalin RM. True 2-d resistivity imaging from vertical electrical soundings to support more sustainable rural water supply borehole siting in Malawi. Appl Sci. 2021;11(3):1-29.
DOI: 10.3390/app11031162
3. Ibraheem IM, El-Qady GM, ElGalladi A. Hydrogeophysical and structural investigation using VES and TDEM data: a case study at El-Nubariya–Wadi El-Natrun area, west Nile Delta, Egypt. NRIAG J Astron Geophys. 2016;5(1):198-215.
DOI: 10.1016/j.nrjag.2016.04.004
4. Salem ZE, El-Bayumy DA. Hydrogeological, petrophysical and hydrogeochemical characteristics of the groundwater aquifers east of Wadi El-Natrun, Egypt. NRIAG J Astron Geophys. 2016;5(1):124-46.
DOI: 10.1016/j.nrjag.2015.12.001
5. Khalil MH. Hydro-geophysical configuration for the quaternary aquifer of Nuweiba alluvial fan. J Environ Eng Geophys. 2010;15(2):77-90.
DOI: 10.2113/JEEG15.2.77
6. Sayed MAA, Shendi EH, Zarif FM. Geoelectrical exploration of the groundwater potentiality around the middle part of Wadi El Natrun- al Alamain road, western Desert, Egypt. Egypt Geophys Soc EGS J. 2009;2(1):75-84.
7. Sandford KS, Arkell WJ. Paleolithic man and Nile valley in lower Egypt. Univ Chicago Oriental Inst Publ. 1939;36:1-105.
8. Said R. The geology of Egypt. Amsterdam and New York: Elsevier. 1962;377.
9. Shata AA, El Fayoumi IF. Geomorphological and morphopedological aspects of the region west of the Nile Delta with special reference to Wadi El-Natrun area. Boll Inst Desert Egypte. 1967; 13(1):1-38.
10. Abu El Izz MS. Landforms of Egypt. Cairo: American University Press. 1971;281.
11. El Shazly EM, Abdel-Hady M, El Ghawaby H, El Kassas K, Khawasik SM, El Shazly MM, et al. Geologic interpretation of Landsat satellite image for west Nile Delta area, Egypt. Cairo: Remote Sensing Center, Academy of Scientific Research and Technology. 1975;38.
12. EMBABY MH, VERBA A. Mean flow properties in the developing region of a circular pipe for turbulent flow at maximum drag reduction. Period Polytech Chem Eng. 1980;24(1):83-92.
13. Embaby AAA. Environmental evaluation for geomorphological situation in relation to the water and soil resources of the region north of the Sadat City, west Nile Delta, Egypt [Ph.D. thesis]. Faculty of Science, Mansoura University; 2003.
14. Shata AA. Geology, in: preliminary report on the geology, hydrogeology and groundwater hydrology of Wadi El Natrun and adjacent areas. part 1. Cairo: Desert Institute, U.A.R. 1962;39.
15. El Fayoumy IF. Geology of groundwater supplies in Wadi El Natrun area [M.Sc. thesis]. Egypt: Faculté Sci. Cairo University. 1964;109.
16. Idris H. Groundwater investigation in Wadi El Natrun. In: Proceedings of the of IAEA symposium, Beirout, Lebanon; 1970;26.
17. Sanad S. Geology of the area between Wadi El-Natrun and the Moghra depression [Ph.D. thesis]. Assuit: Faculty of Science, Assuit University. 1973;184.
18. Omara SN, Sanad S. Rock stratigraphy and structural features of the area between Wadi El Natrun and the Moghra Depression. western Desert, Egypt. Geol., j.b.B16, Hanover, [Ph.D. thesis]. Egypt: Faculty of Science, Ain Shams University. 1975;45-37.
19. El Ghazawi MM. Geological studies of the Quaternary-Neogene aquifers in the area northwest Nile Delta [M.Sc. thesis]. Cairo: Faculty of Science, El Azhar University. 1982;170.
20. Taylor pw, Jones BL. Tertiary studies of Beherira area, northwest Delta region, Egypt. First Break. 1983;1:22-37.
21. Sabagh EAA. Impact land reclam projects groundwater condition area North West Delta [M.Sc. thesis]. Egypt: Faculté Sci, Cairo University. 19921;26p.
22. Sallouma MK, Gomaa MA. Groundwater quality in the Miocene aquifer east and west of Nile Delta and in the north of the Western Desert, Egypt. Ain Shams Sci Bull. 1997;35:47-72.
23. El Shikh AE. Hydrogeology of the area north and west of wadi El Natrun [M.Sc. thesis], Fac. Sc. Shibin El Kom, Egypt: Minufiya University. 2000;177.
24. Khalil A, Mansour K, Rabeh T, Basheer A, Zaher MA, Ali K. Geophysical evaluation for evidence of recharging the Pleistocene aquifer at El-Nubariya Area, West Nile Delta, Egypt. Int J Geosci. 2014;05(3): 324-40.
DOI: 10.4236/ijg.2014.53032

25. Massoud U, Kenawy AA, Ragab EA, Abbas AM, El-Kosery HM. Characterization of the groundwater aquifers at El Sadat City by joint inversion of VES and TEM data. NRIAG J Astron Geophys. 2014;3(2):137-49.
DOI: 10.1016/j.nrjag.2014.10.001
26. Gheorghe A. Processing and synthesis of hydrogeological data. Abacus press. 1979;390.
27. Abd El Baki AA. Hydrogeological and hydro-geochemical studies on the area west of Rosetta branch and south El Nasr Canal; 1983.
28. Ahmed SA. Hydrogeological and isotope assessment of groundwater in Wadi El Natrun and Sadat city, Egypt [Ph.D. thesis]. Cairo: Faculty of Science; 1999.
29. Ahmed MA, Samie SGA, El-Maghrabi HM. Recharge and contamination sources of shallow and deep groundwater of Pleistocene aquifer in El-Sadat industrial city: Isotope and hydrochemical approaches. Environ Earth Sci. 2011; 62(4):751-68.
DOI: 10.1007/s12665-010-0563-x
30. Ibrahim SMM. Groundwater resources management in Wadi El-Farigh and its vicinities for sustainable agricultural development. Cairo: Ain Shams University; 2005.
31. Zohdy AAR, Chapter D1, Application of Surface Geophysics to Ground-Water Investigation. Uni. Stat. Gov. Print. Off. Electrical methods. In: Zohdy AAR, Eaton GP, Mabey DR, editors. 1974;5-66.
32. Telford WM, Geldart LP, Sheriff RE. Applied geophysics. In: Resistivity Method. The Press Syn. of the Uni. of Camb. 1990;535-8.
33. Reynolds JM. An introduction to applied and environmental geophysics. 2nd ed; 2011. p. 2011 John Wiley and Sons Ltd.289345.
34. Kumar D, Krishnamurthy NS. 3D modelling of combination of array results for resistivity profiling data over a dyke for groundwater exploration and development. Environ Earth Sci. 2020;79(17):401.
DOI: 10.1007/s12665-020-09142-9
35. Olorunfemi MO, Ojo JS, Akintunde OM. Hydrogeophysical evaluation of the groundwater potential of the Akure metropolis, southwestern Nigeria. J Min Geol. 1999;35(2):207-28.
36. Kelly WE. Geoelectric sounding for estimating aquifer hydraulic conductivity. Ground Water. 1977;15(6):420-5.
DOI: 10.1111/j.1745-6584.1977.tb03189.x
37. Rahaman MA. Recent advances in the study of the basement complex of Nigeria: Precambrian Geology of Nigeria. GSN. 1988;11-41.
38. Braga ACO, Dourado JC, Malagutti FW. Resistivity (DC) method applied to aquiferprotection studies. Braz J Geophys. 2006;24(4):573-81.
39. Baeckmann W, Schwenk W 1975. Handbook of Cathodic protection. The theory and practice of electrochemical corrosion protection techniques. Portcullis press, Ltd. Surrey, England. 1975;396.
40. Agunloye O. Soil aggressivity along steel pipeline route at Ajaokuta southwestern Nigeria. J Min Geol. 1984;21:97-101.
41. Oladapo M, Mohammed M, Adeoye O, Adetola B. Geoelectrical investigation of the Ondo State housing corporation estate Ijapo Akure, southwestern Nigeria. J Min Geol. 2004;40(1):41-8.
DOI: 10.4314/jmg.v40i1.18807
42. Adeniji AE, Omonona OV, Obiora DN, Chukudebelu JU. Evaluation of soil corrosivity and aquifer protective capacity using geo-electrical investigation inBwari basement area; Abuja. J Earth. 2014; 123(3):491-502.
DOI: 10.1007/s12040-014-0416-1
43. Henriet JP. Direct applications of the Dar Zarrouk parameters in ground water surveys. Geophys Prospect. 1975; 24(3):44-353.
44. WARD SH. Geotechnical and environmental geophysics-no 5. Society of Exploration Geophysicists WARD SH, editor. Resistivity and induced polarization methods. USA. Investigations in Geophysics. 1990;I:147-89.
45. Adegbola RBSO, Oseni ST, Sovi KF, Oyedele LA. Subsurface characterization and its environmental implications using the electrical resistivity survey: case with LASU Foundation Programme Campus, Badagry, Lagos State, Nigeria. Nat Sci. 2010;8(8):146-51.
46. Barker RD. Application of geophysics in groundwater investigations. Water Surv. 1980;84:489-92.
47. El Abd EA. The Geological impact on the water bearing formations in the area south west Nile Delta, Egypt [Ph.D. thesis].

Egypt: Faculté Sci, Menufiya Universidad; 2005.

48. El Fayoumy IF. Geology of the Quaternary Succession and its impact on the groundwater reservoir in the Nile Delta region, Egypt "Submitted to the Ball. Shebin El Kom, Egypt: Faculté Sci. Monoufia Universidad; 1967.
49. El-Fayoumy IF. Geology of groundwater supplies in Wadi El-Natrun area [M.Sc. thesis] Faculty of Science, Cai-ro Univ. Egypt. 1964;109.
50. Kelly WE. Geoelectric sounding for delineating groundwater contamination. Ground Water. 1976;14(1):6-10.
DOI: 10.1111/j.1745-6584.1976.tb03626.x
51. Khalil MH. Hydro-geophysical configuration for the quaternary aquifer of Nuweiba Alluvial Fan. J Environ Eng Geophys (JEEG). 2010;15(2):77-90.
DOI: 10.2113/JEEG15.2.77
52. EMBABY M, MH, VERBA A. Mean flow properties in the developing region of a circular pipe for turbulent flow at maximum drag reduction. Period Polytech Chem Eng. 1980;24(1):83-92:383.
53. Reynolds JM. An introduction to applied and environmental geophysics. John Wiley & Sons; 2011.
54. Sharaky AM, El Hasanein AS, Atta SA, Khallaf KM. Nile and groundwater interaction in the western Nile Delta, Egypt. In: Negm AM, editor. The Nile Delta. Handbook of Environ- mental Chemistry. Vol. 55. Cham: Springer. 2016;33-62.
DOI: 10.1007/698_2016_127
55. Tarabees E, El-Qady G. Seawater intrusion modeling in Rashid area of Nile Delta (Egypt) via the inversion of DC resistivity data. Am J Clim Change. 2016;05(2):147-56.
DOI: 10.4236/ajcc.2016.52014
56. Umar MA, Rafiu AA, Salako K. Evaluation of aquifer protective capacity and soil corrosivity using vertical electrical sounding method in badeggi village, niger state Nigeria Journal of Science, Technology, Mathematics and Education (JOSTMED). 20211;7(1).

Peer-review history:
The peer review history for this paper can be accessed here:
https://www.sdiarticle5.com/review-history/97605